Journal of Agricultural Engineering

https://www.agroengineering.org/

Identification of drought-salinity combined stress in tomato plants by vegetation indices

Alessandro Biglia, Francesco Gresta, Davide Lucien Patono, Lorenzo Comba, Claudio Lovisolo, Paolo Gay, Andrea Schubert

Please cite this article as doi: 10.4081/jae.2024.1599

Submitted: 27 February 2024
Accepted: 29 August 2024

Identification of drought-salinity combined stress in tomato plants by vegetation indices

Alessandro Biglia, Francesco Gresta, Davide Lucien Patono, Lorenzo Comba, Claudio Lovisolo, Paolo Gay, Andrea Schubert

Department of Agricultural, Forest and Food Sciences (DiSAFA), University of Turin, Grugliasco (TO), Italy

Corresponding author: lorenzo.comba@unito.it (L. Comba)

Contributions: all the authors made a substantial intellectual contribution, read and approved the final version of the manuscript, and agreed to be accountable for all aspects of the work.

Disclosure statement: the authors report no conflict of interest.

Acknowledgments: The authors would like to thank Dr. Miquel À. Conesa, Dr. Georgia Ntatsi and Dr. Mathilde Causse for providing the seeds. We also thank Dr. Chiara Agliassa, Dr. Marta Trasoletti, Dr. Daniela Minerdi, and Dr. Giovanni Gamba for their experimental assistance.

Funding: This work was supported by the European Union, PRIMA (Partnership for Research and Innovation in the Mediterranean Area) project VEG-ADAPT ('Adapting Mediterranean vegetable crops to climate change-induced multiple stress'); European Union - NextGenerationEU in the framework of the GRINS -Growing Resilient, INclusive and Sustainable project (GRINS PE00000018 – CUP D13C22002160001); and project NODES which has received funding from the MUR – M4C2 1.5 of PNRR funded by the European Union - NextGenerationEU (Grant agreement no. ECS00000036).

Abstract

A major issue in several farming areas of the Mediterranean basin consists of drought and salinity stress. This stress is mainly due to a steady exposition of warm daily temperature and heatwaves, moreover with inevitable irrigation with saline water. Therefore, detecting the stress is essential to minimise significant yield loss and preserve agricultural sustainability. In this context, remote and proximal sensing can play a crucial role in allowing fast, not destructive, extensive, and reliable assessment of crop status. In this work, the effectiveness of several multispectral indices in detecting salinity and water stress in tomato plants, grown under controlled green-house conditions, was investigated. Three different classifiers (fine tree model, linear discriminant model, and linear support vector machines model) were used to verify whether, and the extent to which, the adopted multispectral indices can be adopted to identify a stress condition of the tomato plants. In the experimental campaign, the stress occurrence on tomato plants was assessed on the base of a set of ecophysiological measurements, such as transpiration, stomatal conductance, and photosynthesis rate. Obtained results showed that a classification model based on linear support vector machines, exploiting the combination of Photochemical Reflectance Index and the Chlorophyl Index, can detect drought and salinity stress in tomato plants with an accuracy higher than 94%.

Keywords: high-throughput phenotyping; close-range remote sensing; multispectral image processing.

Introduction

The Mediterranean Basin has been recognised as one of the most productive horticultural areas, especially for tomatoes (*Solanum lycopersicum* L.). Indeed, tomato cultivation has increased three-fold from the last 50 years, reaching in the European Union (EU) five million hectares in 2015 with more than 85% of tomatoes produced by the Mediterranean members (Eurostat, 2019). Among the non-EU Mediterranean countries, Turkey and Egypt are the most tomato producers with an average production of 10.1 and 7.3 million tons respectively, thus resulting in the fourth and fifth tomato producers in the world (FAOSTAT, 2019).

Because of climate change, some areas of the Mediterranean Basin are increasingly exposed to warm daily temperatures and heatwaves, thus limiting vegetable production (Cramer *et al.*, 2018; Linares *et al.*, 2020; Tramblay *et al.*, 2020). Therefore, within the next few years, drought stress is likely to become an essential issue for Mediterranean farmers, impacting the yield and productivity of the crop (Liu *et al.*, 2016). Also, in some Mediterranean coastal regions, salinity stress has been receiving much attention due to the unavoidable use of saline water for irrigation, which causes significant yield loss and important modifications in the soil physicochemical properties promoting its degradation (Paranychianakis *et al.*, 2005; Aragüés *et al.*, 2011).

Drought and salinity stress are involved in limiting plant growth and yield, mainly due to loss of turgor, impaired enzymatic activity, stomata closure and consequent less carbon intake in plants, downregulation of photosynthesis, damage in the photosynthesis machinery caused by Reactive Oxygen Species (ROS) increment, sodium (Na^+) toxicity, and nutrient imbalance especially Nitrogen (NO^{2-}) (Chaves *et al.*, 2003; Chaves *et al.*, 2009; Farooq *et al.*, 2012; Ors and Suarez, 2017; Ekinci *et al.*, 2018).

One of the most valuable techniques to assess the physiological status of plants under stress is the measurement of photosynthesis with gas exchange systems. This technique has been developed and applied for several decades and considered the qualitative reference for photosynthetic measurements (Patono *et al.*, 2022, 2023). In gas exchange systems, a leaf (or the whole plant canopy) is compartmentalised inside a cuvette, and a known airflow rate conveyed through the cuvette to measure CO_2 and H_2O concentration of air entering and leaving the cuvette. From the data obtained in gas exchange systems, the most common measurements that can be evaluated are net photosynthetic rate or assimilation rate (A), transpiration rate (E), stomatal conductance (G_s) and CO_2 concentration inside the leaf substomatal cavity (C_i). The rate of net fixed moles of CO_2 and of H_2O exchanged between the leaf and the atmosphere are respectively A and E. Stomatal conductance, which represents how easily vapor can pass through stomata, is calculated as the ratio between E and the vapor pressure deficit (VPD). VPD is the difference between the saturation water vapor pressure at the temperature and pressure of the atmosphere at which plant is exposed and the actual water vapor pressure of the atmosphere at the moment of measurement. The CO_2 concentration inside the leaf, if G_s and the external concentration of CO_2 remain constant, reflects the CO_2 flux from outside to the site of carboxylation (von Caemmerer and Farquhar, 1981).

However, there are many challenges that do not allow an extensive use of gas exchange systems in precision agriculture management frameworks; these include high investment costs, time needed to ensuring good quality measurements, difficulties to scale photosynthetic parameters from few leaves to the whole plant, and difficulty in automating data acquisition (Siebers, 2021). In this context, remote sensing based on optical sensors can play a crucial role in allowing fast, not destructive, extensive, and high spatial and temporal resolution

measurements of crop status with respect to standard photosynthetic methods, especially in greenhouses and open fields (Usha and Singh, 2013; Katsoulas *et al.*, 2016). Optical sensors usually detect canopy transmittance (Tantinantrakun *et al.*, 2023), reflectance, or emissivity (Lioy *et al.*, 2021) signals, from which both agronomic information and physiological traits about the crop can be extracted. Multispectral cameras are commonly employed to detect canopy reflectance. The intensity of the reflectance signal depends on several parameters such as the morphological properties of the leaves, branches and stems, light absorption by pigments, and plant architecture (Winterhalter *et al.*, 2013). Since photosynthesis is a function of chlorophyll abundance and activity, measurement of light absorption by this pigment provides a link between optical remote sensing measurements and plant photosynthetic status (Schlemmer *et al.*, 2013).

Several vegetation indices have been adopted to describe crop characteristics (e.g., leaf area index, biomass, yield) and impact of stresses (e.g., water, nutrient, pests and diseases) using multispectral bands as input (Sinclair and Ludlow, 1986; Comba *et al.*, 2019, 2020; Guidoni *et al.*, 2021; Psiroukis *et al.*, 2022). However, there are still information gaps regarding the relationship between the data acquired through gas exchange systems and multi-spectral vegetation indices. First, an integrative approach with physiological data directly assessed on plants is required to assess by these indices the real plant performance under stress (Usha and Singh, 2013). Second, previous works on multispectral-based detection of drought and salinity stress have been focused on the evaluation of one single stress only, without considering the possibility of combined stress, such as drought and salinity. Finally, it is still poorly understood how the multispectral parameters can be effective in standardising the early detection of the stress in distinct genotypes, considering their differential responses to the stress.

The specific objective of this study is the identification of vegetation indices obtained from multispectral imagery that allow the classification of drought- and salt-stressed or unstressed tomato plants in a fast, cost effective and non-invasive way. Indeed, the use of classification methods based on vegetation indices has the great advantage of saving time with respect to the direct measurement of leaf gas exchange.

Materials and Methods

Combined drought and salinity stress

The experimental campaign was conducted under greenhouse conditions, and tomato (*Solanum lycopersicum* L.) varieties Moneymaker, de Ramellet, ATS-048/06, Ολυμπία (Olympia), ECU1067 (Cherry) and Mex-104 (Cherry) were considered. Accessions were sown in plastic seedlings trays filled with peat and then placed in a walk-in growth chamber set at 26 °C, 50% of relative humidity, and 100 µmol m^{-2} s^{-1} PAR. When three-week old, tomato plants were transplanted into square plastic pots of 13 cm height and 0.75 dm^3 volume containing perlite; the pots were then transferred to a greenhouse. During the experimental period, the average temperature in the greenhouse was 25.5±3.8°C and the relative humidity 77.0 ± 23.0 %. The environmental data were collected with a data logger (Tinytag Plus 2 - TGP 4500, Gemini Data loggers Ltd, Chichester, UK) placed inside the greenhouse.

The experimental design was set up as complete randomised blocks and included 12 conditions (6 accessions × 2 treatments), each represented by 3 replicate pots. To this aim, 36 pots were prepared. Pots with unstressed plants were marked as Tu (18 plants), while those with stressed plants Ts (18 plants). In addition, to assess the effect of the evapotranspiration phenomena from the perlite soil, 6 pots without plants (3 respectively for the unstressed and stressed condition) were filled with perlite only. Before the combined drought and salinity stress treatment, which was planned to last 3 weeks, all 42 pots were saturated with water and drained for 24 hours, in order to let them reach common initial conditions of field capacity.

Each pot was then connected to an automatic sprinkler system with drippers, previously installed in the greenhouse. Unstressed plants received 2 minutes of irrigation 4 times per day, while stressed plants received 1 minute of irrigation once per day. The water flow per pot was 25 mL min^{-1}, and the drippers functioning was daily checked for both stressed and unstressed lines by collecting and measuring water delivered by randomly selected drippers.
In order to assess the effectiveness of water stress imposition, the relative transpiration TR_{k} of each stressed plant was evaluated once a week. The parameter TR_{k} is defined as the ratio between the transpiration of stressed plants and the average of the ones belonging to the corresponding unstressed group (Sinclair and Ludlow, 1986). More in detail, the procedure published in Sinclair and Ludlow (1986) to compute the relative transpiration TR_{k} of the k^{th} stressed plant is

$$TR_{\mathrm{k}} = \frac{MTs_{\mathrm{k,j}} - MTs_{\mathrm{k,j-1}}}{N^{-1} \cdot \sum_{\mathrm{i}=1}^{N} \left(MTu_{\mathrm{i,j}} - MTu_{\mathrm{i,j-1}}\right)}, \tag{1}$$

where $MTs_{\mathrm{k,j}}$ and $MTs_{\mathrm{k,j-1}}$ are the weights of the stressed pot Ts_{k} on j-th day and the day before (j-1), respectively, while MTu_{j} and $MTu_{\mathrm{j-1}}$ are the weights of each unstressed pot MTu, belonging to the same accessions category (genotype in this case). Finally, N represents the number of replicates (pots) in the accessions category. In this work, Eq. (1) was modified to take into account two phenomena affecting the relative transpiration computation in the experimental campaign: (1) the perlite properties of high porosity and low water retention, and (2) the effect of the evapotranspiration phenomena of the soil. For the first aspect, the amount of water applied to pots W and the drained water from pots D were weighed and considered. For the second aspect, weights MP of pots with only perlite were also taken into account. The resulting TR_{k} equation was thus

$$TR_{\mathrm{k}} = \frac{MTs_{\mathrm{k,j}} - \left(MTs_{\mathrm{k,j-1}} + Ws_{\mathrm{j-1}} - Ds\right) - \left[MPs_{\mathrm{j}} - \left(MPs_{\mathrm{j-1}} + Ws_{\mathrm{j-1}} - DMPu\right)\right]}{N^{-1} \cdot \sum_{\mathrm{i}=1}^{N} \left\{\left(MTu_{\mathrm{i,j}} - MTu_{\mathrm{i,j-1}}\right) - \left(Wu_{\mathrm{j-1}} - Du_{\mathrm{j-1}}\right) - \left[MPu_{\mathrm{j}} - \left(MPu_{\mathrm{j-1}} + Wu_{\mathrm{j-1}} - DMPs\right)\right]\right\}}, \tag{2}$$

where $Ws_{\mathrm{j-1}}$ and $Wu_{\mathrm{j-1}}$ represent the grams of water applied the day before (j-1) to stressed and unstressed pots, respectively, and Ds and Du represent the grams of water drained from stressed and unstressed pots. MP are the weight of pots filled with perlite only, which were watered as those in the unstressed (MPu) and stressed (MPs) plants classes and the drainage also from these pots (DMPu and $DMPs$) were collected and considered in the final calculation, as described before. $Ws_{\mathrm{j-1}}$ and $Wu_{\mathrm{j-1}}$ were measured by randomly collecting the water from the drippers in the appropriate day.
In order to provide sufficient nutrients to the plants during all the experimental period, a fertirrigation with a standard De Kreij *et al.* (1997) solution was performed three times per week. To induce salinity stress, the water-stressed plants were fertigated with a standard De Kreij et al. (1997) solution, three times per week, in which 81 mM of commercial sea salt was dissolved, thus resulting in a final electrical conductivity (EC) of about 8 dS m^{-1}. Commercial sea salt was preferred to pure NaCl salt in order to simulate seawater infiltration in the irrigation system as suggested by De Pascale et al. (2003). Finally, in order to monitor the perlite salinity, the drainages of plant pots were randomly collected, and the EC was measured with an electrical conductivity meter.

Ecophysiological measurements

After 3 weeks of drought and salinity stress treatments, when the average transpiration ratio (TR) and electrical conductivity (EC) of all stressed accessions was 0.31 ± 0.06 and 5.23 ± 0.13 dS m^{-1} respectively, CO_2 gas exchange measurements on stressed and un-stressed plants were performed to calculate the assimilation rate (A), transpiration rate (E), stomatal conductance (G_s) and CO_2 concentration inside the leaf (C_i). To this aim, a GFS-3000 IRGA (Walz, Germany) instrument was used, which measures CO_2 and H_2O gas exchange between plant and ambient air in a controlled environment. Measurements were made on a sunny day between 10 am and 1 pm, and were done on three leaves for each tomato plant. For each measurement, a well expanded leaf of was clamped in a cuvette of 8 cm^2. An air flow of 750 µmol s^{-1} was maintained inside the cuvette. Temperature and relative humidity of the fluxing air were set to follow greenhouse condition. During the entire measurement campaign (10 am - 1 pm), temperature and relative humidity ranged between 20 and 24 °C, and 60 and 80 % respectively. The cuvette was irradiated by a GFS-3000 LED lamp at a constant light intensity of 300 µmol photons m^{-2} s^{-1}. A waiting time of 90 s was adopted to allow instrument purge time and leaf acclimatisation after the leaf was clamped, thus reaching stable values of ΔCO_2 and ΔH_2O. After the purge time, 30 consecutive recordings at 1 s interval were performed. The average value of the 30 time points was used in the gas exchange equations described in von Caemmerer and Farquhar (1981) to calculate the assimilation rate A, transpiration rate E, stomatal conductance G_s and concentration inside the leaf C_i. Stressed and unstressed plants were measured alternately, and, at the end of the measurements, plants were introduced in the multispectral images acquisition system for multispectral measurements.
To verify the effectiveness of the induced stress conditions, the correlation between the measured ecophysiological measurements was investigated based on a regression analysis in Matlab® R2022a environment, where the best fitting curves were obtained. Specifically, the A and G_s measurements were plotted against the E and C_i ones respectively.

Multispectral images acquisition system

In order to evaluate vegetation indices of stressed and unstressed plants, multispectral imagery of each treated pot has been acquired. To this aim, a MAIA S2 multispectral camera (SAL Engineering, Russi (RA), Italy) was adopted, which features an array of nine sensors with 1.2 MPx resolution. Each sensor has a dimension of 4.8 x 3.6 mm with a pixel size of 3.75 µm, and the spectral coverage is from 390 to 950 nm (average spectral resolution of 37 nm). Please refers to Table 1 for MAIA S2 spectral bands. The MAIA camera is equipped with a global shutter technology which allows pixels charge collection of the nine sensors to be started simultaneously, thus the nine images can be acquired in "one shot" with a perfect synchronisation among bands with a frame rate set to 1 Hz. This technical solution also avoids the so-called negative Jello effect that occurs when acquiring an image at a high-frequency rate. Moreover, the fast exposure time of the nine global shutters guarantees the absence of the blurring. The images were saved in a proprietary format in 12 bits.
The MAIA camera was installed face down on the roof of a closed box having a wooden frame, at a relative height of 2.50 metres from the ground. The frame had a square shape with an edge and height of 3 and 4 metres respectively. The artificial illumination system consisted of six halogen lamps of 100 W each and a light diffuser. The six lamps were mounted on the roof of the box and a shield was installed around the MAIA camera in order to prevent possible direct light from the lamps to the nine sensors. The developed data acquisition system was also equipped with a RGB camera to automatically acquire an image of the unique identificative QR code applied on each pot. After the acquisition of a multispectral image of the plant, the system also performs a scanning procedure with a 3D sensor and a turning platform, with the

aim to reconstruct a 3D model of the plant (not used in this work). The schematic representation of the acquisition system is reported in Figure 1.
The inner side surfaces and the floor of the box were upholstered with matte white and matte black material respectively to avoid the shadow effect. Indeed, each pot was in the centre of the floor before acquiring the multispectral image. An Incident Light Sensor (ILS) was integrated with the MAIA camera and mounted inside the box to measure the light level for each shot in each band. The ILS allowed both data for correction due to light level and true reflectance ratios calculation to be collected. The ILS data were automatically stored into the log file related to the image acquisition set.
The raw multispectral images were then processed with the MAIA images software MultiCam Stitcher Pro for geometric correction, coregistration and radiometric correction in order to obtain images in .tiff format. Four black and white chessboards, printed on A5 size paper, were attached to the floor of the box to help in the coregistration process.
Each plant was placed in the middle of the box floor and both the MAIA and the illumination system were controlled by Matlab® script using an Arduino shield as I/O device, to menage automatic triggers. Considering all the steps (plant positioning in the box, acquiring images and plant removing), each multispectral image took about 2 minutes to be automatically acquired and saved.

Vegetation indices

Multispectral imaging is a powerful tool for agronomic analysis as it allows plant status to be monitored in a non-destructive way and with a high temporal resolution. After images acquisition and correction (see paragraph *Multispectral images acquisition system*), the images segmentation was performed to separate leaves from the background by using a semantic segmentation method in Matlab® R2022a environment based on a convolutional neural network (U-net) and deep learning (Comba *et al.*, 2020; Biglia *et al.*, 2022). Since this method looks at the entire set of multispectral channels, it has a higher accuracy than traditional methods based on a fixed threshold. After segmentation, a mask for each plant was automatically created to identify only the area covered by the leaves (young and developed) as shown in Figure 2. Then, the mask was applied to all the 9 bands of the multispectral imagery to extract the reflectance values of the regions of interest.
The vegetation indices calculated and evaluated in this work for the identification of tomato plants under combined drought and salinity stress are listed in Table 2. The nine indices were selected according to literature review on applications of crops reflectance monitoring for drought and/or salinity stress detection (Katsoulas *et al.*, 2016; Elvanidi *et al.*, 2018). For each of the 36 nadiral multispectral images acquired, the selected nine vegetation indices were computed for all the pixels considered in the ROI (leaves) and then the average value was computed, which was considered as representative of each single tomato plant canopy. The false colour representation of PRI index computation for two sample plants, one from each group, is reported in Figure 2.

VIs-based stress detection

In order to define a VIs-based robust classifier to detect combined drought and salinity stress condition of tomato plants, an explorative analysis of the potential informative content of each considered vegetation index was firstly assessed. In this phase, two methods have been applied: (1) the Principal Component Analysis (PCA) and the Analysis of Variance (ANOVA). More in details, the PCA, which was performed on the entire dataset (36 plants/observations and 9 VIs/variables), allows to quantify the variance explained and to detect those VIs providing more informative content on the dataset variance. Then, the ANOVA was applied

on the values of each vegetation index individually, considering the induced stresses as groups. This additional preliminary analysis was used to further characterise the dataset and to select most performing indices to be used in the subsequent phase. Indeed, the two best vegetation indices are selected, among the nine analysed, and used to test three different classifiers, (i) decision tree model, (ii) discriminant analysis, and (iii) support vector machine. All the data processing was performed and implemented in Matlab® R2022a environment. The *k-fold* cross-validation technique, with k=6, was used in the implemented Matlab® algorithms to verify the absence of over-fitting during the models training (Arlot and Celisse, 2010).

Results

Ecophysiological measurements

Results of the computed relative transpiration TR, calculated by Equation 2, and of the measured electrical conductivity EC, showed a significance difference between the unstressed pots compared to the stressed ones (Table 3), confirming the effectiveness of the used stress protocol.

The regression between the measurements of the assimilation rate A and the transpiration rate E are well approximated by the following exponential equation

$$A = -15.08exp^{-0.803E} + 11.17\,, \tag{3}$$

with a coefficient of determination of 0.81. The graphical represented of Eq. (3) is reported in Figure 3, together with the experimental measurements. Unstressed plants present (blue points in Figure 3), on average, higher values of A and E than stressed plants (red squares in Figure 3). The following exponential equation, plotted in Figure 4,

$$G_s = 1.992e^{-7}exp^{0.047C_i} + 7.192exp^{0.008C_i} \tag{4}$$

approximates the regression model between the G_s (stomatal conductance) and C_i (CO_2 concentration inside the leaf) measurements. Unstressed plants (blue points in Figure 4) have, on average, higher values of both G_s and C_i than stressed plants which are represented with red squares in Figure 4.

Vegetation index based stress detection

Results of the PCA explorative analysis of the entire VIs dataset are graphically reported in Figure 5. The higher absolute values of the first principal component coefficients were obtained by CRI and CI indices (defined in Table 2), with 0.73 and 0.55 respectively. VOGREI was the third, with a coefficient value of 0.39, while all the other VIs contributed to the first principal component with coefficients lower than 0.05.

The values of the vegetation indices computed for each pot of the experimental campaign are graphically represented by boxplots in Figure 6, grouped by unstressed and stressed plants. The potential informative content about combined drought and salinity stress, of each considered vegetation index, was then assessed by Analysis of Variance (ANOVA). Results of ANOVA confirmed that the CI and PRI indices, which scored the two lowest p-values of $0.0079\text{x}10^{-6}$ and $0.0006\text{x}10^{-9}$ respectively, are the most performing ones, and they are thus adopted in the subsequent phase to detect the optimal VIs-based stress detection classifier.

Results of the three tested classification methods to detect the tomato plants affected by stress condition are reported in Figures 7-9, for decision tree model, discriminant analysis model, and support vector machine (SVM) model, respectively. In particular, solid red and blue markers represent correctly classified tomato plants as stressed (true positive) and unstressed

(true negative) respectively, while red and blue empty markers represent incorrectly classified tomato plants (false positive and false negative).
The confusion matrices related to the results of Figures 7-9 are shown in Tables 4-6. It can be noticed that the decision tree model has lower performance in correctly classify the tomato plants to stress and unstressed category than the other two models (Figure 7, Table 4). The performance of this model in detecting unstressed tomato plants is slightly higher than 90% while the one to detect stressed tomato plants is nearly 90%. The linear discriminant model has both performances to correctly classify unstressed and stressed tomato plants higher than 90% (Figure 8, Table 5). The last classification method tested, the SVM model, has detected with 100% accuracy the unstressed plants and with almost 90% the stressed ones (Figure 9, Table 6).

Discussion and conclusions

The experimental protocol was able to induce a mild combined drought and salinity stress (E of 0.5-2 mmol m^{-2} s^{-1}) (Secchi *et al.*, 2013) in stressed tomato plants, with an average relative transpiration ratio (TR) of around 0.3 and a perlite with electrical conductivity (EC) of around 5 dS m^{-1}. In addition, it can be noted that G_s values for stressed plants do not increase with increasing of the C_i values (Figure 4). Indeed, in mild stress conditions, regulation of photosynthesis is due to combined action of stomatal and metabolic limitations, consequently the CO_2 concentration inside the leaves varies widely based on metabolic feedbacks to stomatal regulation. The exponential equation well combines a theoretical fully stomatal response (a putative vertical interpolation line) with a theoretical pure metabolic response (a putative horizontal interpolation line). The former response could be seen in the higher performing outliers of unstressed plants, the latter in the lower performing outliers of plants under stress. In the intermediate region of the exponential curve all the transition states mix, as described.
For what concert the vegetation index based stress detection, the most remarkable result is that the relation between the photochemical reflectance index (PRI) and chlorophyll index (CI) obtained from multispectral imagery allows the classification of stressed or unstressed tomato plants in a fast, cost effective and non-invasive way. Indeed, the use of classification methods based on vegetation indices has the great advantage of saving time with respect to the evaluation of ecophysiological measurements. The combined drought and salinity stress not only leads to stomatal closure but also decreases the photosynthesis rate and causes reduced growth, thus leading to the loss of key pigments such as chlorophylls (Chaves *et al.*, 2009). Chlorophylls are the main actors in the absorption of light for the photochemical reaction in plants, and the reflectance stress induced by chlorosis is high in the range of 690-700 nm (Carter, 1993). On the other hand, the PRI index is related to the overall plant canopy pigments, and carotenoids in particular (Roberts *et al.*, 2012). Carotenoids are involved in the absorption of light for photosynthesis and have the important role to protect chlorophylls during a combined drought and salinity stress (Chaves and Oliveira, 2004). This requires the rapid interconversion of the carotenoid xanthophyll to zeaxanthin (Krause and Weis, 1991), which competes with photochemistry of absorbed light by dissipating the energy as heat, a process called Non-Photochemical Quenching (NPQ) (Demmig-Adams and Adams, 1996). From a spectral point of view, carotenoid interconversion is recorded with a decrease in reflectance at 531 nm. So, stressed plants are characterised by lower PRI values than unstressed plants.
The system and algorithms used for multispectral image acquisition and processing respectively were effective for the identification of tomato plants undergoing a combined drought and salinity stress at an early growth stage (4 weeks from transplant). The results presented in Figures 7-9, as well as in Tables 4-6, indicate that some vegetation indices

combined with deep learning tools allow a good identification of stressed tomato plants. These innovative tools based on multispectral imaging were indeed selected and developed to identify stressed plants avoiding the use of time-consuming traditional techniques based on ecophysiological measurements.
In conclusion, the methodology here presented involved consecutive steps to stress the tomato plants in a controlled environment, monitor their ecophysiological parameters with a traditional method and then acquire multispectral images for vegetation indices computation. The tomato plant imaging system was automatic and non-destructive, and allowed stressed plant to be classified with a very good accuracy, higher than 90%, by using a deep learning approach in Matlab® environment.
To the best of our knowledge, assessing the possibility of using multispectral imaging to automatically extract information from tomato plants under combined stress conditions (drought and salinity) has not been investigated yet. In addition, the developed image processing steps could be profitably applied to imageries of other plant species. Moreover, the MAIA S2 multispectral camera, besides its original development for aerial images, fulfills the requirements to be also used in the field installed on fixed platforms or robotic platforms with a short distance from the crop. The developed methodology to detect combined draught and salinity stress can be easily applied in a real productive structured context, such as commercial greenhouses, implementing e.g. a mobile gantry to host the optical spectral sensor. The adoption in open field has additional difficulties to be managed, such as the absence of facilities and the need to couple the sensor with amore complex displacement system, such as UGVs.

References

Aragüés, R., Urdanoz, V., Çetin, M., Kirda, C., Daghari, H., Ltifi, W., et al. 2011. Soil salinity related to physical soil characteristics and irrigation management in four Mediterranean irrigation districts. Agr. Water Manage. 98:959-966.

Arlot, A., Celisse, A. 2010. A survey of cross-validation procedures for model selection. Statist. Surv. 4:40-79.

Biglia, A., Zaman, S., Gay, P., Ricauda Aimonino, D., Comba, L. 2022. 3D point cloud density-based segmentation for vine rows detection and localization. Comput. Electron. Agr.199:107166.

Carter, G.A. 1993. Responses of leaf spectral reflectance to plant stress. Am. J. Bot. 80:239-243.

Chaves, M.M., Maroco, J.P., Pereira J.S. 2003. Understanding plant responses to drought - from genes to the whole plan". Funct. Plant Biol. 30:239-264.

Chaves, M.M., Oliveira, M.M. 2004. Mechanisms underlying plant resilience to water deficits: Prospects for water-saving agriculture. J. Exp.l Bot. 55:2365-2384.

Chaves, M.M., Flexas, J., Pinheiro, C. 2009. Photosynthesis under drought and salt stress: Regulation mechanisms from whole plant to cell. Ann. Bot. 103:551-560.

Comba, L., Biglia, A., Ricauda Aimonino, D., Barge, P., Tortia, C., Gay, P. 2019. 2D and 3D data fusion for crop monitoring in precision agriculture. 2019 IEEE International Workshop on Metrology for Agriculture and Forestry (MetroAgriFor), Portici, Italy. pp. 62-67.

Comba, L., Biglia, A., Ricauda Aimonino, D., Barge, P., Tortia, C., Gay, P. 2021. Thermal network clustering for crops thermal mapping. Acta Hortic. 1311:513-520.

Comba, L., Zaman, S., Biglia, A., Ricauda Aimonino, D., Dabbene, F., Gay, P. 2020. Semantic interpretation and complexity reduction of 3D point clouds of vineyards. Biosyst. Eng. 197:216-230.

Cramer, W., Guiot, J., Fader, M., Garrabou, J., Gattuso, J.-P., Iglesias, A., et al. 2018. Climate change and interconnected risks to sustainable development in the Mediterranean. Nature Clim. Change 8:972-980.
De Kreij, C., Voogt, W., Van den Bos, A.L., Baas, R. 1997. [Voedingsoplossingen voor de teelt van tomaat in gesloten teeltsystemen].[in Dutch]. Brochure VG Tomaat, The Netherlands.
Demmig-Adams, B., Adams, W. 1996. The role of xanthophyll cycle carotenoids in the protection of photosynthesis. Trends Plant Sci. 1:21-26.
De Pascale, S., Ruggiero, C., Barbieri, G., Maggio, A. 2003. Physiological responses of pepper to salinity and drought. J. Am. Soc. Hortic. Sci. 128:48-54.
Ekinci, M., Ors, S., Turan, M., Yildiz, S., Yildirim, E. 2018. Effects of individual and combined effects of salinity and drought on physiological, nutritional and biochemical properties of cabbage (Brassica oleracea var. capitata). Sci. Hortic.-Amsterdam 240:196-204.
Elvanidi, A., Katsoulas, N., Ferentinos, K.P., Bartzanas, T., Kittas, C. 2018. Hyperspectral machine vision as a tool for water stress severity assessment in soilless tomato crop. Biosyst. Eng. 165:25-35.
Eurostat. 2019. European Commission. Available from: https://ec.europa.eu/eurostat
FAOSTAT. 2019. Food and agriculture data. Available from: htttp://fao.org/faostat
Farooq, M., Hussain, M., Wahid, A., Siddique, K.H.M. 2012. Drought stress in plants: An overview. In: Aroca, R. (ed.), Plant responses to drought stress. Berlin, Springer.
Guidoni, S., Drory, E., Comba, L., Biglia, A., Ricauda Aimonino, D., Gay, P. 2021. A method for crop water status evaluation by thermal imagery for precision viticulture: preliminary results. Acta Hortic. 1314:83-90.
Katsoulas, N., Elvanidi, A. Ferentinos, K.P., Kacira, M., Bartzanas, T., Kittas, C. 2016. Crop reflectance monitoring as a tool for water stress detection in greenhouses: A review. Biosyst. Eng.151:374-398.
Krause, G.H., Weis, E. 1991. Chlorophyll fluorescence and photosynthesis: the basics. Annu. Rev. Plant Physiol. Plant Mol. Biol. 42:313-349.
Linares, C., Díaz, J., Negev, M., Martínez, G.S., Debono, R., Paz, S. 2020. Impacts of climate change on the public health of the Medi-terranean Basin population - Current situation, projections, preparedness and adaptation. Environ. Res. 182:109107.
Lioy, S., Bianchi, E., Biglia, A., Bessone, M., Laurino, D., Porporato, M. 2021. Viability of thermal imaging in detecting nests of the invasive hornet Vespa velutina. Insect Sci. 28:271-277.
Liu, E.K., Mei, X.R., Yan, C.R., Gong, D.Z., Zhang, Y.Q. 2016. Effects of water stress on photosynthetic characteristics, dry matter translocation and WUE in two winter wheat genotypes. Agr. Water Manage. 167:75-85.
Ors, S., Suarez, D.L. 2017. Spinach biomass yield and physiological response to interactive salinity and water stress. Agr. Water Manage. 190:31-41.
Paranychianakis, N.V, Chartzoulakis, K.S. 2005. Irrigation of Mediterranean crops with saline water: from physiology to management practices. Agr. Ecosyst. Environ. 106:171-187.
Patono, D.L., Eloi Alcatrão, L., Dicembrini, E., Ivaldi, G., Ricauda Aimonino, D., Lovisolo, C. 2023. Technical advances for measurement of gas exchange at the whole plant level: Design solutions and prototype tests to carry out shoot and rootzone analyses in plants of different sizes. Plant Sci. 326:111505.
Patono, D.L., Said-Pullicino, D., Eloi Alcatrão, L., Firbus, A., Ivaldi, G., Chitarra, W., et al. 2022. Photosynthetic recovery in drought-rehydrated grapevines is associated with high demand from the sinks, maximizing the fruit-oriented performance. Plant J. 112:1098-1111.

Psiroukis, V., Darra, N., Kasimati, A., Trojacek, P., Hasanli, G., Fountas, S. 2022. Development of a multi-scale tomato yield prediction model in Azerbaijan using spectral indices from Sentinel-2 imagery. Remote Sens. 14:4202.

Roberts, D., Roth, K., Perroy, R. 2012. Hyperspectral vegetation indices. In: Huete, A, Lyon, J.G., Thenkabail, P.S. (eds.), Hyperspectral Remote Sensing of Vegetation. CRC Press. pp. 309-327.

Schlemmer, M., Gitelson, A., Schepers, J., Ferguson, R., Peng, Y., Shanahan, J., et al. 2013. Remote estimation of nitrogen and chlorophyll contents in maize at leaf and canopy levels. Int. J. Appl. Earth Obs. Geoinf. 25:47-54.

Secchi, F., Perrone, I., Chitarra, W., Zwieniecka, A.K., Lovisolo, C., Zwieniecki, M.A. 2013. The dynamics of embolism refilling in abscisic acid (ABA)-deficient tomato plants. Int. J. Mol. Sci. 14:359-377.

Siebers, M.H., Gomez-Casanovas, N., Fu, P., Meacham-Hensold, K., Moore, C.E., Bernacchi, C.J. 2021. Emerging approaches to measure photosynthesis from the leaf to the ecosystem. Emerg. Top. Life Sci. 5:261-274.

Sinclair, T.R., Ludlow, M.M. 1986. Influence of soil water supply on the plant water balance of four tropical grain legumes. Aust. J. Plant Physiol. 13:329-341.

Tantinantrakun, A., Sukwanit, S., Thompson, A.K., Teerachaichayut, S. 2023. Nondestructive evaluation of SW-NIRS and NIR-HSI for predicting the maturity index of intact pineapples. Nondestructive evaluation of SW-NIRS and NIR-HSI for predicting the maturity index of intact pineapples. Postharvest Biol. Technol.195:112141.

Tramblay, Y., Koutroulis, A., Samaniego, L., Vicente-Serrano, S.M., Volaire,F., Boone, A., et al. 2020. Challenges for drought assessment in the Mediterranean region under future climate scenarios. Earth-Sci. Rev. 210:103348.

Usha, K., Singh, B. 2013. Potential applications of remote sensing in horticulture - A review. Sci. Hortic.-Amsterdam 153:71-83.

von Caemmerer, S., Farquhar , G.D. 1981. Some relationships between the biochemistry of photosynthesis and the gas exchange of leaves. Planta 153:376-387.

Winterhalter, L., Mistele, B., Schmidhalter, U. 2013. Evaluation of active and passive sensor systems in the field to phenotype maize hybrids with high-throughput. Field Crops Res. 154:236-245.

Table 1. Wavelength ranges of MAIA S2 bands.

Band name	Band range
Violet	$B1 = 433 - 453\ [nm]$
Blue	$B2 = 457.5 - 522.5\ [nm]$
Green	$B3 = 525 - 575\ [nm]$
Red	$B4 = 650 - 680\ [nm]$
Red Edge 1	$B5 = 697.5 - 712.5\ [nm]$
Red Edge 2	$B6 = 732.5 - 747.5\ [nm]$
Near Infrared 1	$B7 = 773 - 793\ [nm]$
Near Infrared 2	$B8 = 784.5 - 899.5\ [nm]$
Near Infrared 3	$B9 = 855 - 875\ [nm]$

Table 2. Vegetation indices selected in this study.

Type index	Index name	Index formula
Simple ratio	Anthocyanin Reflectance Index	$ARI = \frac{B5}{B3}$
	Chlorophyll Index	$CI = \frac{B7}{B3} - 1$
	Carotenoid Reflectance Index	$CRI = \frac{B5}{B2}$
	Plant Senescence Reflectance Index	$PSRI = \frac{B4 - B2}{B6}$
	Vogelmann Red Edge Index	$VOGREI = \frac{B6}{B5}$
Normalised difference	Green Normalised Differential Vegetation Index	$GNDVI = \frac{B7 - B3}{B7 + B3}$
	Normalised Differential Red Edge Index	$NDVI = \frac{B7 - B5}{B7 + B5}$
	Normalised Pigment Chlorophyll Index	$NPCI = \frac{B4 - B1}{B4 + B1}$
	Photochemical Reflectance Index	$PRI = \frac{B2 - B3}{B2 + B3}$

Table 3. Experimental conditions between unstressed and stressed pots. Each value represents the average of eighteen pots with Standard Deviation. ANOVA one-way statistical significance is indicated by an asterisk (*) symbol.

	TR	EC (dS m^{-1})
Unstressed	1±0.023	0.53±0.029
Stressed	0.31±0.063 ***	5.23±0.13 ***

Table 4. Confusion matrix of the fine tree classification model (see Figure 6).

True	unstressed	88.9 %	11.1 %
class	stressed	5.6 %	94.4 %
		unstressed	stressed
		Predicted class	

Table 5. Confusion matrix of the linear discriminant classification model (see Figure 7).

True	unstressed	94.4 %	5.6 %
class	stressed	5.6 %	94.4 %
		unstressed	stressed
		Predicted class	

Table 6. Confusion matrix of the linear support vector machines classification model (see Figure 8).

True	unstressed	94.4 %	5.6 %
class	stressed	0 %	100 %
		unstressed	stressed
		Predicted class	

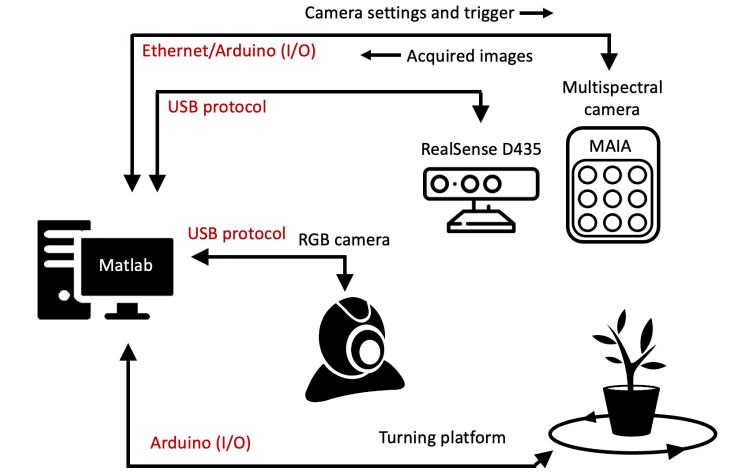

Figure 1. Scheme of the developed acquisition system for plant multispectral images and 3D point cloud model (not exploited in this work).

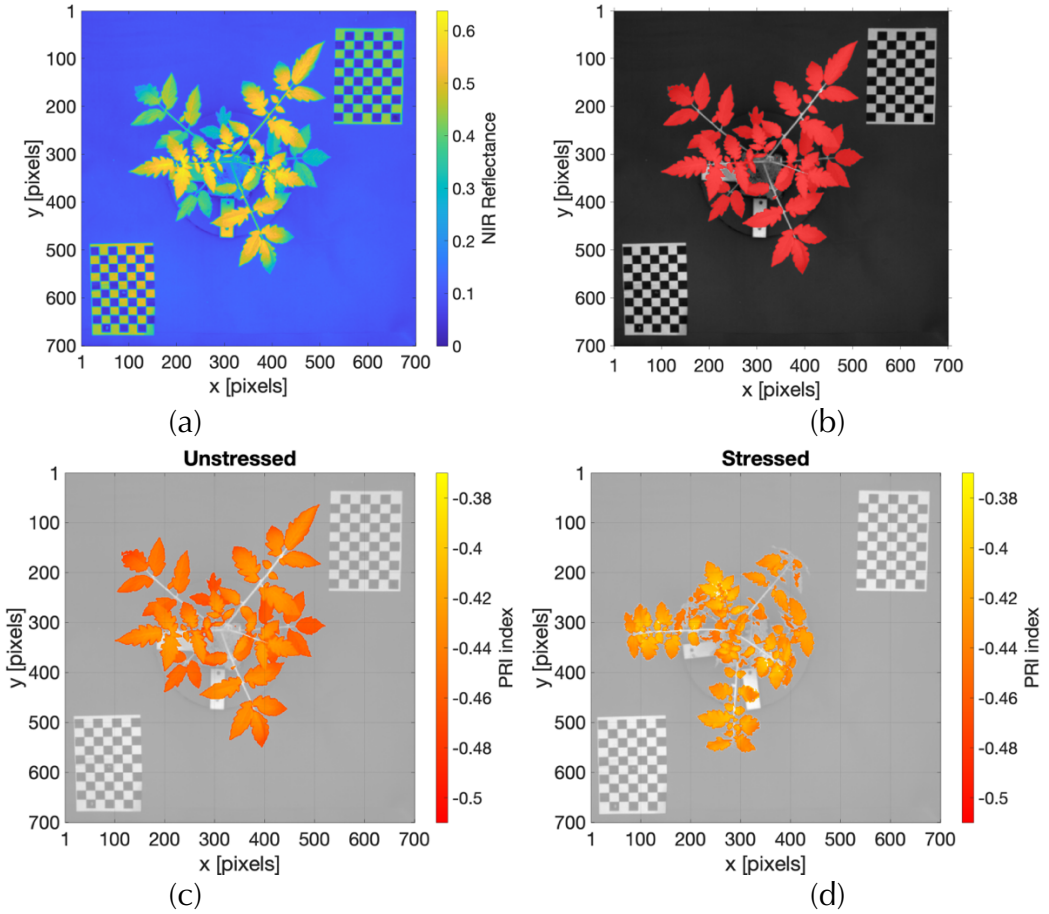

Figure 2. (a) False colour visualisation of the NIR band image of a tomato plant acquired by the MAIA S2 camera (B7, Table 1), (b) results of the image segmentation to detect pixels representing tomato leaves (red), and false colour visualization of PRI index (Table 2) of unstressed (c) and stressed (d) sample plant.

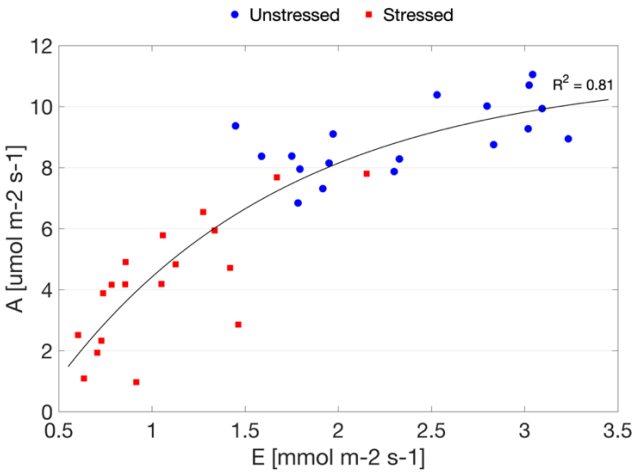

Figure 3. Ecophysiological measurements of unstressed (blue dots) and stressed (red squares) tomato plants: assimilation rate (A) as a function of the transpiration rate (E). The black solid line represents the data regression model, with its coefficient of determination (R^2), see Eq. (3).

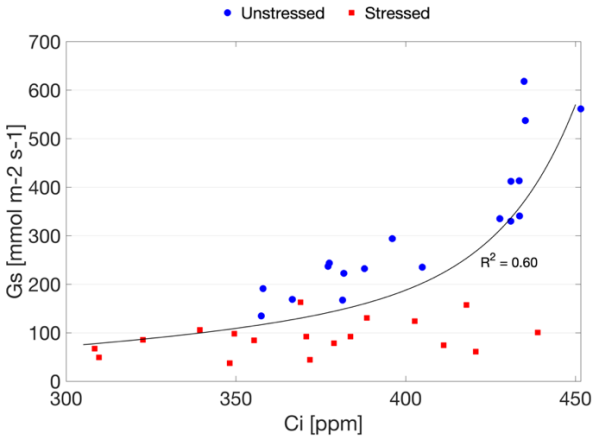

Figure 4. Ecophysiological measurements of unstressed (blue dots) and stressed (red squares) tomato plants: the stomatal conductance (G_s) as a function of the concentration inside the leaf (C_i). The black line represents the data regression model with its coefficient of determination (R^2), see Eq. (4).

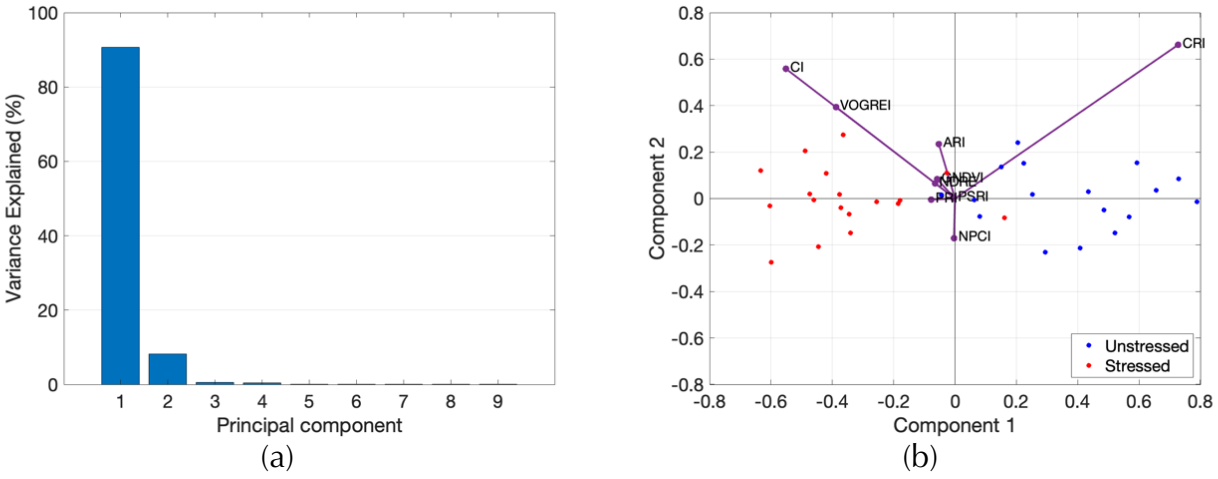

Figure 5. Results of PCA analysis applied on the entire VIs dataset: (a) percentage of variance explained by each principal component and (b) scatter plot of obtained observations scores in the plane of first two principal components, together with orthonormal principal component coefficients for each variable (VIs).

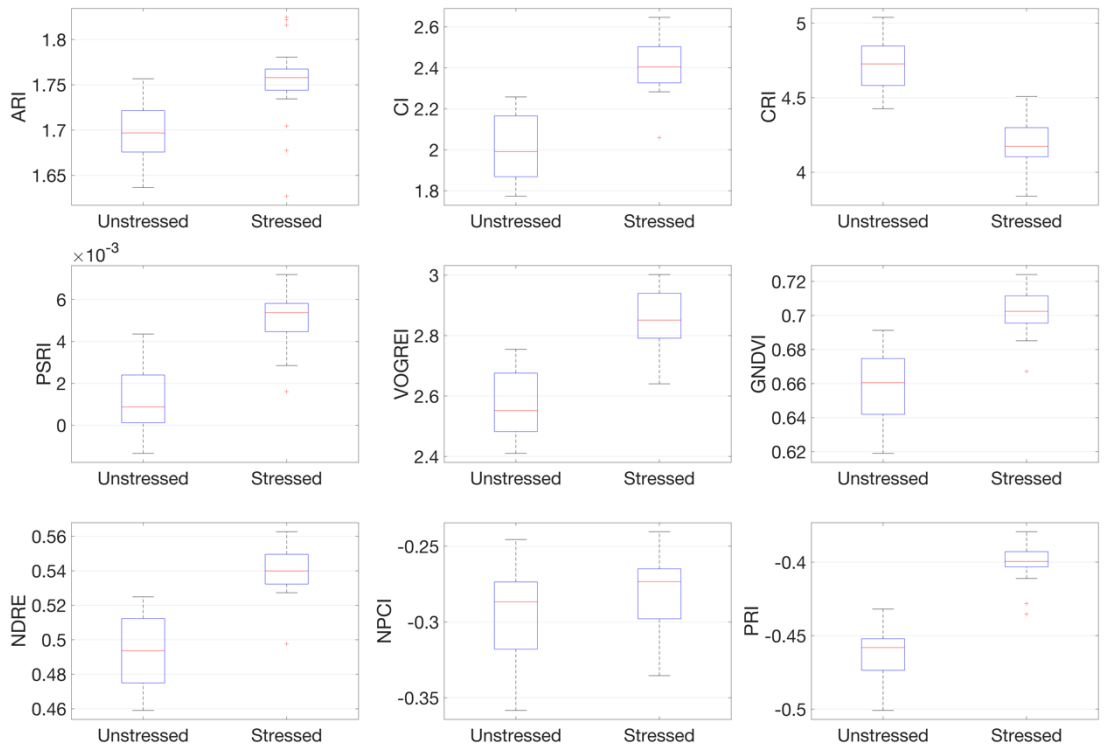

Figure 6. Values of the vegetation indices listed in Table 2, separately calculated for unstressed and stressed plants. Each boxplot was made considering eighteen vegetation indices values.

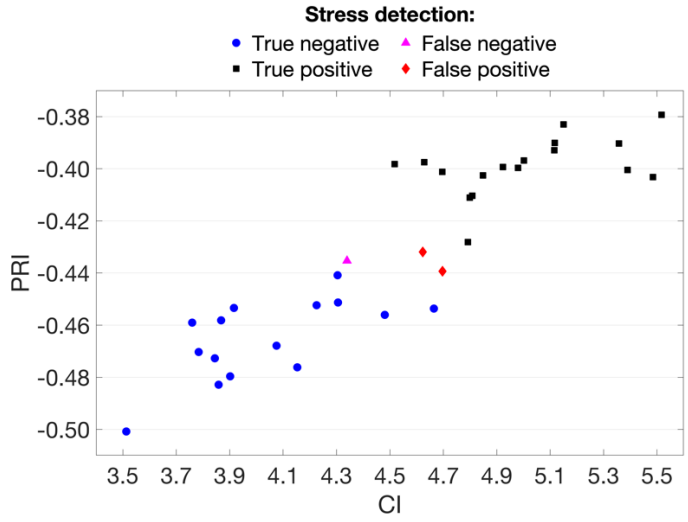

Figure 7. Results of the decision tree classification model based on the photochemical reflectance index (PRI) and the chlorophyll index (CI). Red and blue circles represent correctly classified tomato plants as stressed (true positive) and unstressed (true negative), red and blue triangles represent incorrectly classified tomato plants (false positive and false negative).

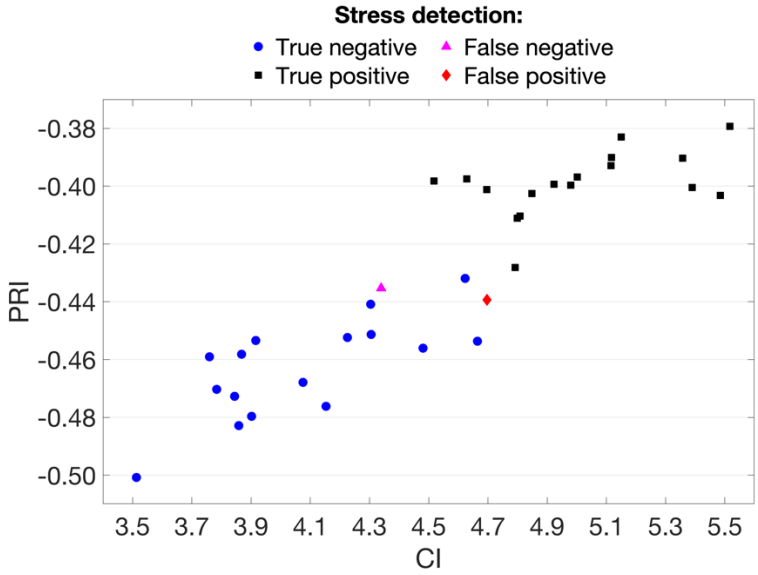

Figure 8. Results of the linear discriminant classification model based on the photochemical reflectance index (PRI) and the chlorophyll index (CI). Red and blue circles represent correctly classified tomato plants as stressed (true positive) and unstressed (true negative), red and blue triangles represent incorrectly classified tomato plants (false positive and false negative).

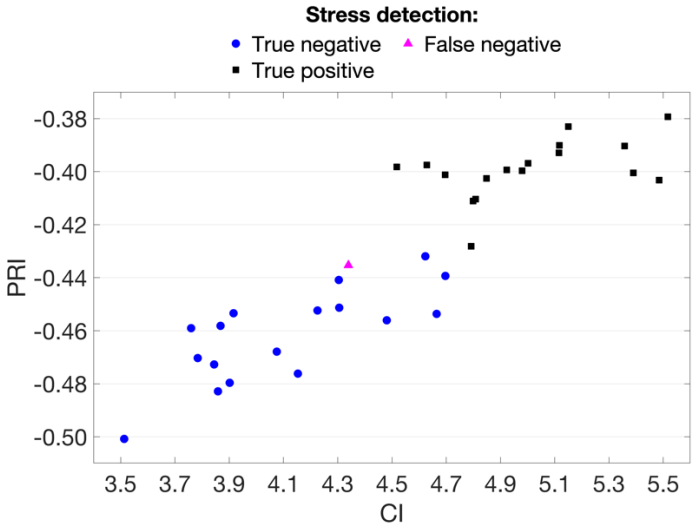

Figure 9. Results of the linear support vector machines classification model based on the photochemical reflectance index (PRI) and the chlorophyll index (CI). Red and blue circles represent correctly classified tomato plants as stressed (true positive) and unstressed (true negative), red and blue triangles represent incorrectly classified tomato plants (false positive and false negative).